Magnetic behaviour in the spin-density-wave phase of $Cr_{1-x}Mn_x$ (x < 20% Mn) alloys

1996 J. Phys.: Condens. Matter 8 7925

(http://iopscience.iop.org/0953-8984/8/42/012)

J. Phys.: Condens. Matter **8** (1996) 7925–7940. Printed in the UK

Magnetic behaviour in the spin-density-wave phase of $Cr_{1-x}Mn_x$ ($x < 20\%$ Mn) alloys

V Yu Galkin†¶, P C de Camargo†, N Ali‡ and E Fawcett§

† Physics Department, UFPR, Curitiba, Brazil
‡ Physics Department, Southern Illinois University, Carbondale, IL, USA
§ Physics Department, University of Toronto, Toronto, Canada

Received 29 May 1996

Abstract. The magnetic susceptibilities χ of twelve samples in the alloy system $Cr_{1-x}Mn_x$, with x ranging from $\ll 0.1$ to 19.4% Mn, are measured in the temperature range $5 \leqslant T \leqslant 300$ K, in applied fields in the range $30 \leqslant H \leqslant 1000$ Oe, after cooling in zero field and in the measuring field. The field dependence of the magnetization $M(H)$ is measured at $T = 5$ K in the range $-55 \leqslant H \leqslant 55$ kOe. The magnetic behaviour is characteristic of a spin glass, with hysteresis of $M(H)$ and also hysteresis between the field-cooled and zero-field-cooled states, a peak in $\chi(T)$ for the zero-field-cooled state, and relaxation of M as the logarithm of time when H is changed at low temperature. Unlike a typical spin glass, however, the peak in $\chi(T)$ in the zero-field-cooled state is at roughly the same temperature (between 25 and 40 K) for all concentrations, and Curie–Weiss paramagnetism is seen at higher temperatures only for $x \geqslant 7.7\%$ Mn. The Curie constant increases by an order of magnitude between $x = 11.2$ and 13.5% Mn, corresponding perhaps to a change in the atomic short-range order.

1. Introduction

The alloys $Cr_{1-x}Mn_x$ are antiferromagnetic (AFM) across the whole phase diagram from pure Cr to Mn. Maki and Adachi [1] found that, for $x < 10\%$ Mn, the magnetic susceptibility $\chi(T)$ is essentially constant in the spin-density-wave (SDW) phase for a large temperature interval below the Néel temperature T_N, while for higher Mn concentrations $\chi(T)$ obeys a Curie–Weiss (CW) law. In all the alloys, $\chi(T)$ decreases monotonically with increasing T above T_N, and was described as obeying a CW law for all concentrations [1, 2]. Maki and Adachi made the broad generalization that this behaviour in the SDW phase corresponds at higher Mn concentrations to localized magnetic moments that do not interact with the SDW, while at lower concentrations the Pauli paramagnetism results from 'the antiferromagnetic band being filled up by itinerant electrons supplied from substituted Mn atoms'. They also found, for $x < 15\%$ Mn, a remarkable anomaly in the temperature dependence of the magnetic susceptibility $\chi(T)$ in a field $H = 2.7$ kOe, and nonlinearity in the field dependence of the magnetization $M(H)$ with hysteresis, for $x < 2\%$ Mn.

We have re-examined the magnetic behaviour of this alloy system in the SDW phase with the greatly enhanced sensitivity available with a SQUID magnetometer. This permits the use of small measuring fields, which has revealed that the anomaly in the temperature dependence of $\chi(T)$ has some characteristics of a spin glass, namely: hysteresis with respect

¶ On leave from I P Bardin Central Research Institute for Ferrous Metallurgy, 107055, 2 Baumanskaya 9/23, Moscow, Russia.

0953-8984/96/427925+16$19.50

to field cooling, with the irreversibility limit between the zero-field-cooled (ZFC) and field-cooled (FC) states dropping to lower temperatures with increasing field; hysteresis with respect to field cycling; relaxation of the magnetization as the logarithm of time when the applied field is changed at low temperature, at a rate in the ZFC state considerably faster than in the FC state; and remanent magnetization [3].

There are, on the other hand, some very significant differences between the behaviour of CrMn alloys and that of the prototypical spin glass CuMn [4]. First, the characteristic temperature of the anomaly is roughly the same, between about 40 and 80 K, over the whole concentration range from a trace of Mn ($x \ll 0.1\%$) to 19.4% Mn. Secondly, Pauli paramagnetism is seen over a wide temperature range above the anomaly for the lower concentrations of Mn, and CW paramagnetism only appears for $x \geqslant 6.2\%$ Mn. For $x \geqslant 13.5\%$ Mn, the Curie constant is an order of magnetism larger than it is in the range $7.7 \leqslant x \leqslant 11.2\%$ Mn, so that in the higher-concentration alloys the CW paramagnetism dominates the low-temperature anomaly, which is considerably weaker than at lower concentrations.

The results for dilute $Cr_{1-x}Mn_x$ alloys containing up to 4.6% Mn were reported previously [3]. The present paper reports measurements on alloys up to $x = 19.4\%$ Mn. This demonstrates the wide range of compositions over which spin-glass effects are observed, from a trace of Mn to beyond this composition, and also shows that in this range two other interesting regimes of magnetic behaviour exist in the CrMn system: from $7 \leqslant x \leqslant 12\%$ Mn, where the susceptibility $\chi(T)$ above the spin-glass pinning temperature obeys a CW law, but the magnetization in high fields at low temperature is only a little larger than at lower concentrations of Mn; and for $x \geqslant 12\%$ Mn, where the Curie constant increases by almost an order of magnitude, as does the low-temperature magnetization.

2. Experiment

The twelve $Cr_{1-x}Mn_x$ samples range in composition from $x \ll 0.1$ to 19.4% Mn (all compositions are in atomic per cent). The sample described as having $x \ll 0.1\%$ Mn contains only a trace of Mn, and the Néel temperature T_N is not appreciably greater than that of pure Cr. Ingots weighing about 70 g of the required composition were melted in a vacuum-arc furnace in an argon atmosphere, and then crystallized on a water-cooled copper plate. They were remelted five times to achieve homogeneity, vacuum annealed for 24 h at a temperature of 1050 °C, and then quenched. The actual composition of some samples was determined by inductively coupled plasma atomic-emission spectroscopy, while that of others was estimated from T_N, with the knowledge of $T_N(x)$ thus obtained. The value of T_N was determined from the anomaly in the temperature dependence of the thermal expansion (to be published).

Some conventional structural characterization was performed by use of Auger spectroscopy on some of the samples, which indicated satisfactory compositional homogeneity, but the best measure of this is the fact that it was possible in all cases to observe the anomaly in the thermal expansion at the Néel temperature, whose value varies rapidly with Mn content in this range. The magnetization M was measured with a SQUID magnetometer from Quantum Design in San Diego. The temperature dependence of magnetic susceptibility, defined as $\chi(T) = M(T)/H$, was measured in the temperature range $5 \leqslant T \leqslant 300$ K. $\chi(T)$ was measured with increasing T, both after cooling in zero magnetic field H (the ZFC state) and after cooling in the measuring field (the FC state), which was in the range $30 \leqslant H \leqslant 1000$ Oe. A pure Cr sample was also measured for reference purposes.

The field dependence of the magnetization $M(H)$ was measured at temperature $T = 5$ K, in the field range $-55 \leqslant H \leqslant 55$ kOe. The relaxation of the magnetization as a function of time over several hours was measured after changing the applied field for two samples, but relaxation effects were not studied systematically.

3. Results

The most remarkable feature of the magnetic behaviour of $Cr_{1-x}Mn_x$ alloys is the sharp rise in the magnetic susceptibility $\chi(T)$ at some temperature $T < 100$ K, followed by a maximum, which is seen clearly in the zero-field-cooled state for samples containing $x \leqslant 11.2\%$ Mn, being weaker in samples of higher Mn concentration. This is illustrated variously in figures 1(a), 2, 4, 5 and 7, with the size $\Delta\chi$ of the maximum as a function of concentration being shown in figure 3(a). With decreasing temperature below the maximum, $\chi(T)$ measured in small fields of $H = 30$ or 80 Oe falls towards zero at zero temperature (figures 1(a) and 4), but in a large magnetic field of $H = 1000$ Oe the fall is weak (figures 2 and 5).

For samples containing smaller concentrations of Mn, $x \leqslant 1.5\%$ Mn, the onset of the low-temperature peak is well defined and the peak is sharp (figure 4(a)–(c)). It is still possible to define clearly a 'pinning temperature' to characterize the onset of the peak for $x = 3.1\%$ Mn (figure 4(d)), but for $x = 6.2\%$ Mn there seem to be two breaks in the slope of the curve $\chi(T)$, which suggest the existence of two pinning temperatures (figure 4(e)). For larger concentrations of Mn the upper pinning temperature is relatively well defined (figures 1(a) and (b)) remains fairly constant up to $x = 19.4\%$ Mn (table 1).

Table 1. Temperature dependence of the susceptibility of $Cr_{1-x}Mn_x$ alloys for $x \geqslant 7.7\%$ Mn expressed in terms of the parameters for a fit to a CW law above pinning temperature T_p.

x % Mn	A (10^{-6} emu g^{-1})	C (10^{-6} K emu g^{-1})	T_0 (K)	T_p (K)
7.7	3.2	235	−190	80
10.1	3.5	274	−180	73
11.2	3.6	219	−130	77
13.5	2.9	1960	−150	75
14.7	2.7	2130	−170	65
19.4	3.4	1420	−130	67

The shape of the peak in $\chi(T)$ is apparently related to the nature of the spin-density wave, since the phase diagram of $Cr_{1-x}Mn_x$ [5] shows that the SDW is incommensurate at low temperature for an Mn concentration less than about 2% Mn, and commensurate for larger concentrations.

Above the pinning temperature T_p, the magnetic susceptibility $\chi(T)$ increases slowly with temperature up to $T = 300$ K for $Cr_{1-x}Mn_x$. This weak dependence on temperature is described as Pauli susceptibility in figure 3(b).

For larger concentrations, $x \geqslant 7.7\%$ Mn, $\chi(T)$ is temperature dependent above T_p and follows closely a CW law:

$$\chi = \chi_0 + \frac{C}{T - T_0}. \tag{1}$$

This is indicated in figure 3(a), where the size of the low-temperature peak in $\chi(T)$ is shown as a function of Mn concentration.

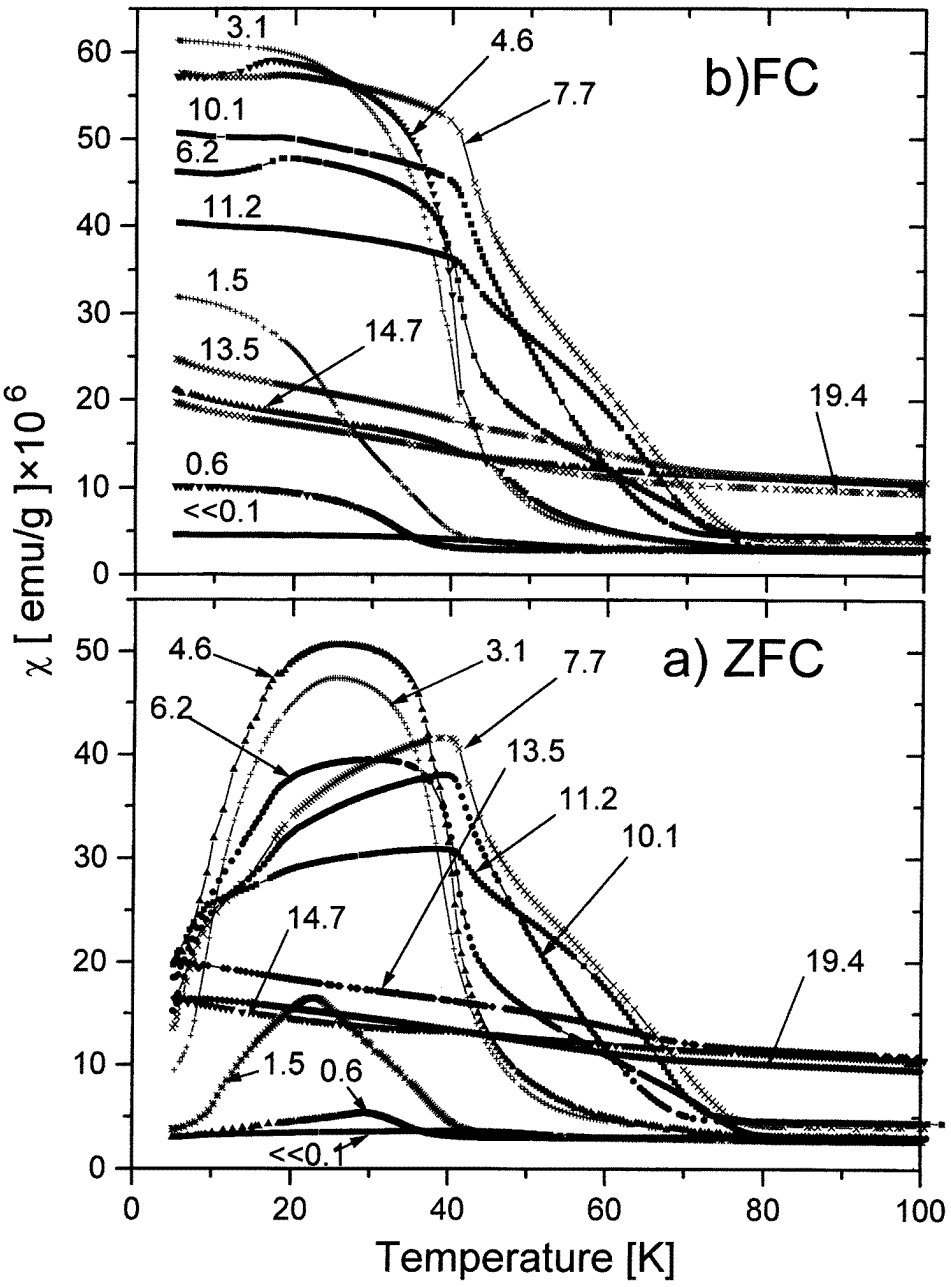

Figure 1. The temperature dependence of the magnetic susceptibility $\chi(T)$ of $Cr_{1-x}Mn_x$ alloys: (a) in the ZFC state; and (b) in the FC state, with a measuring field $H = 80$ Oe, over the temperature range $5 \leqslant T \leqslant 100$ K. The curves are labelled with the concentration of Mn, x%.

The CW parameters are given in table 1. The Curie constant C increases by about an order of magnitude between the concentrations 11.2 and 13.5% Mn, as shown in figure 3(a).

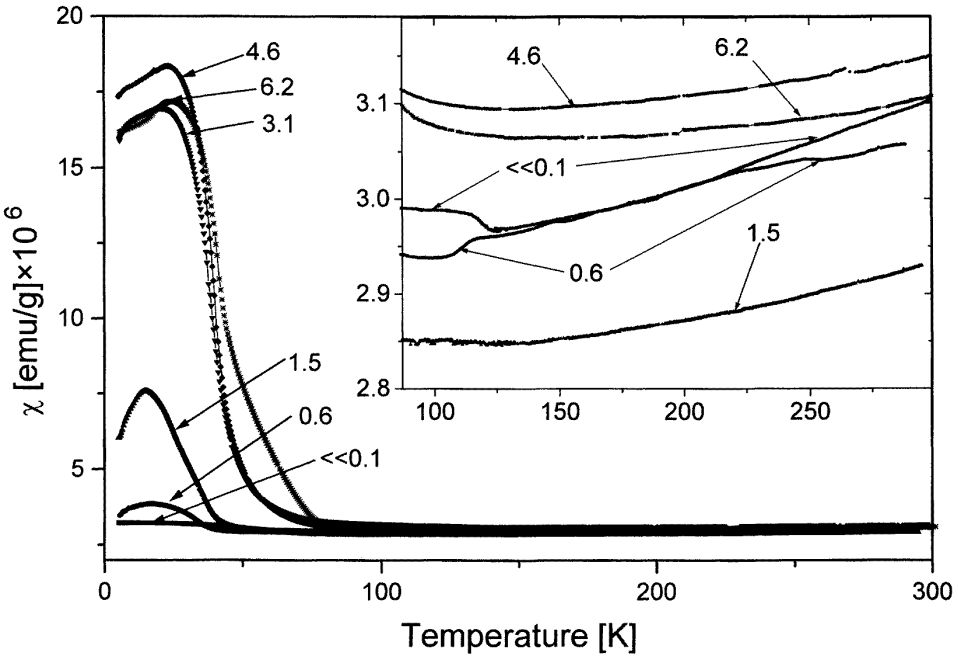

Figure 2. The temperature dependence of the magnetic susceptibility $\chi(T)$ of $Cr_{1-x}Mn_x$ alloys in the ZFC state, with a measuring field $H = 1000$ Oe, over the temperature range $5 \leqslant T \leqslant 300$ K. The inset shows the behaviour above $T = 80$ K, with an expanded ordinate scale. The curves are labelled with the concentration of Mn, x%.

This is related to the fact that the three samples containing the largest amounts of Mn have a considerably larger high-field differential magnetic susceptibility than the samples with Mn concentration $x \leqslant 11.2\%$ Mn, as illustrated in figures 3(b) and 10(b). The low-temperature peak in $\chi(T)$ starting at about the same pinning temperature, $T_p \approx 80$ K, is seen in these samples in the ZFC state as shown for the Cr+13.5% Mn sample in figure 7. But it is reduced greatly in magnitude relative to the peak in the lower-Mn-concentration samples (figure 3(a)), and appearing together with the large CW paramagnetism the maximum almost becomes a shoulder on the $\chi(T)$ curve (figure 7). It is noteworthy that the fit of the data for $\chi(T)$ for these samples to a CW law is very good over a wide temperature interval, as shown in figure 8.

Another feature of the temperature dependence of $\chi(T)$, illustrated in the inset to figure 2, is the appearance of an anomaly at about $T = 120$ K for $x \ll 0.1$ and 0.6% Mn, which the phase diagram [5] shows must be related to the spin-flip phase transition. This is a first-order transition between the transverse and longitudinal phases, where we observed a step in the $\chi(T)$ curve in pure Cr also, as seen in figure 6. The step in $\chi(T)$ for the $x \ll 0.1\%$ Mn sample is opposite in sign to that for the $x = 0.6\%$ Mn sample, and the magnitude of each is somewhat larger than that of the step in pure Cr. Similar behaviour is seen in the susceptibility at the spin-flip transition in dilute $Cr_{1-x}V_x$ single crystals [6]. A proper study of this effect would require measurements of the components of the susceptibility tensor in single-crystal samples in a state having a single SDW wavevector (see table V in [7]).

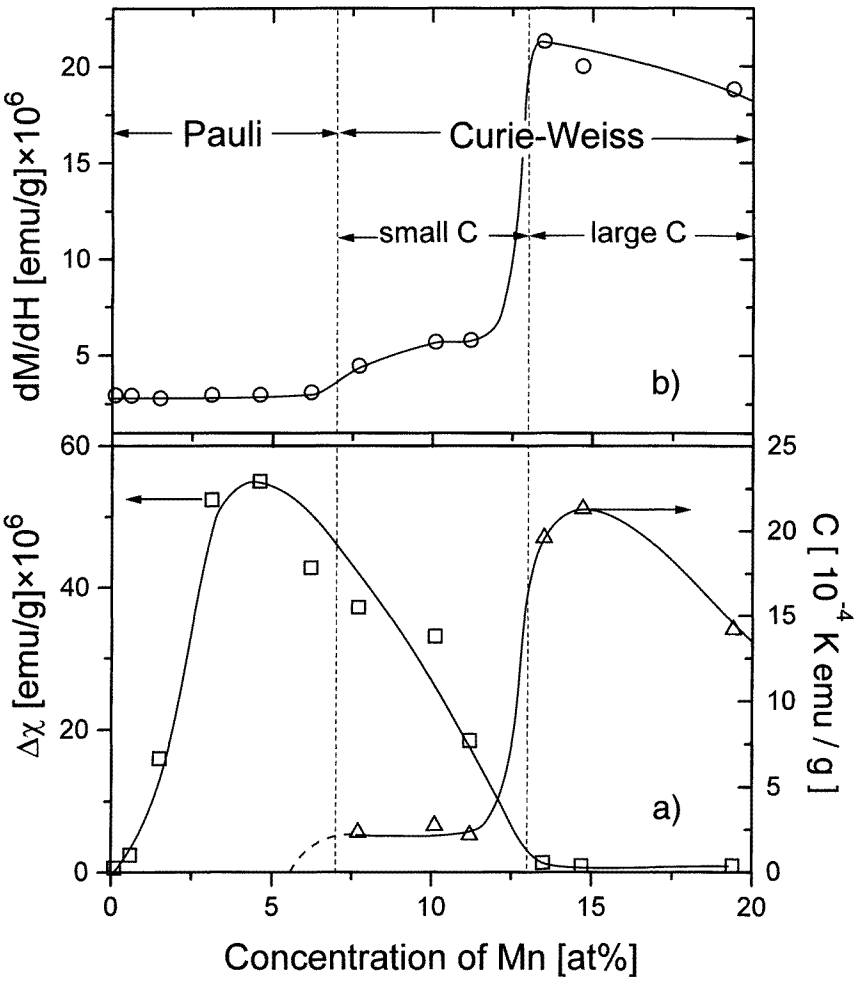

Figure 3. The variation in $Cr_{1-x}Mn_x$ alloys with the concentration of Mn, x%, of several quantities characterizing the magnetic behaviour: (a) □: the magnitude of the peak height $\Delta\chi$ of the low-temperature anomaly in the magnetic susceptibility $\chi(T)$ in the ZFC state, with measuring field $H = 30$ Oe, obtained by subtracting the background value extrapolated from above the pinning temperature (left-hand scale) (the concentration ranges over which different regimes of $\chi(T)$ are observed are shown in panel (b)), △: the Curie constant C in a fit of $\chi(T)$ to a CW law (right-hand scale); and (b) ○ : the differential susceptibility dM/dH for $H \geqslant 5$ kOe.

There is also a discontinuity in the slope of the $\chi(T)$ curve for the Cr+0.6% Mn sample at a temperature, $T \simeq 225$ K, which coincides with the transition for this composition from the low-temperature incommensurate SDW to the commensurate SDW phase [5]. This phase transition is well known to be strongly first order and hysteretic [8], so that a measurement of $\chi(T)$ with decreasing temperature should show the same anomaly at $T \simeq 200$ K. The transition was first observed in the same sample by means of thermal expansion by Kondorskii *et al* [9].

It is interesting to note that in the ternary alloy, (Cr+1.3% Si)+0.6% Mn, for which

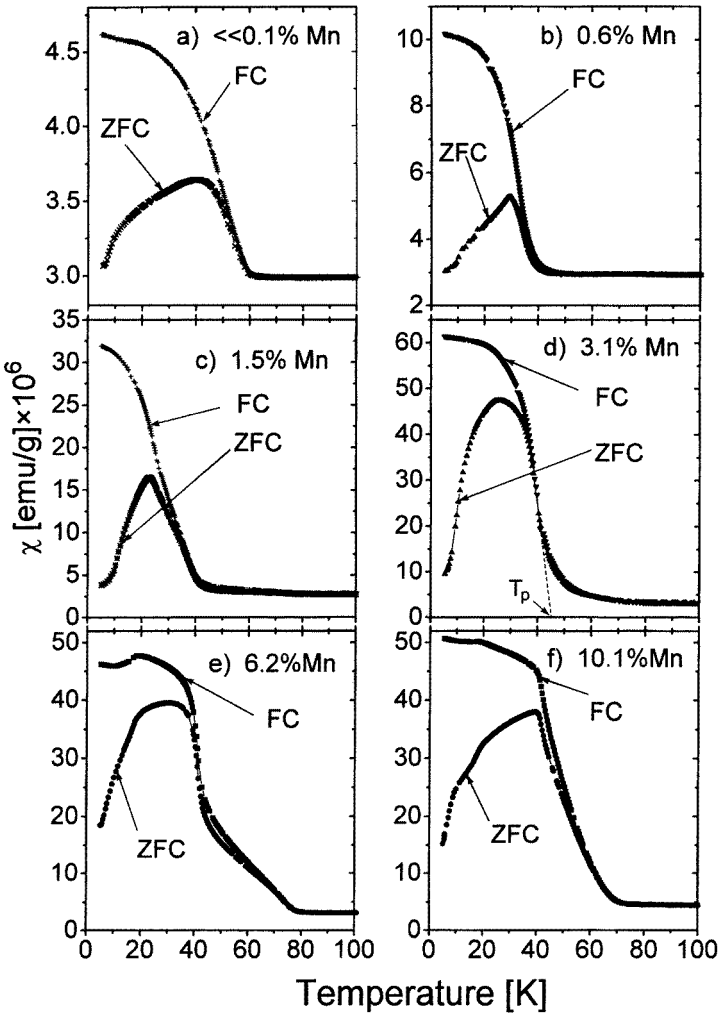

Figure 4. The temperature dependence of the magnetic susceptibility $\chi(T)$ for $Cr_{1-x}Mn_x$ alloys having compositions from $x \ll 0.1$ to 10.1% Mn, with the results for the ZFC and FC states for each being displayed in the same panel to facilitate comparison. The measuring field is $H = 80$ Oe. The method used to define the pinning temperature T_p is illustrated in panel (d).

measurements of the magnetic susceptibility were previously reported [3], the SDW phase is commensurate at all temperatures below T_N, and the slope of $\chi(T)$ in the same temperature range is essentially the same as it is in the commensurate SDW of Cr+0.6% Mn.

We now turn to the features observed in our samples that lead us to believe that the $Cr_{1-x}Mn_x$ system constitutes a new type of spin glass [3]. We see in figure 4 that CrMn alloys show two characteristic features of a spin glass, namely, the peak in the temperature dependence of the magnetic susceptibility $\chi(T)$ in the ZFC state, and the hysteresis when the sample is field cooled in the measuring field. In a typical metallic spin glass, in which the RKKY interaction between the magnetic impurity atoms is responsible for their frustration, the peak in the ZFC curve is identified as the freezing temperature T_f, which in CuMn, for

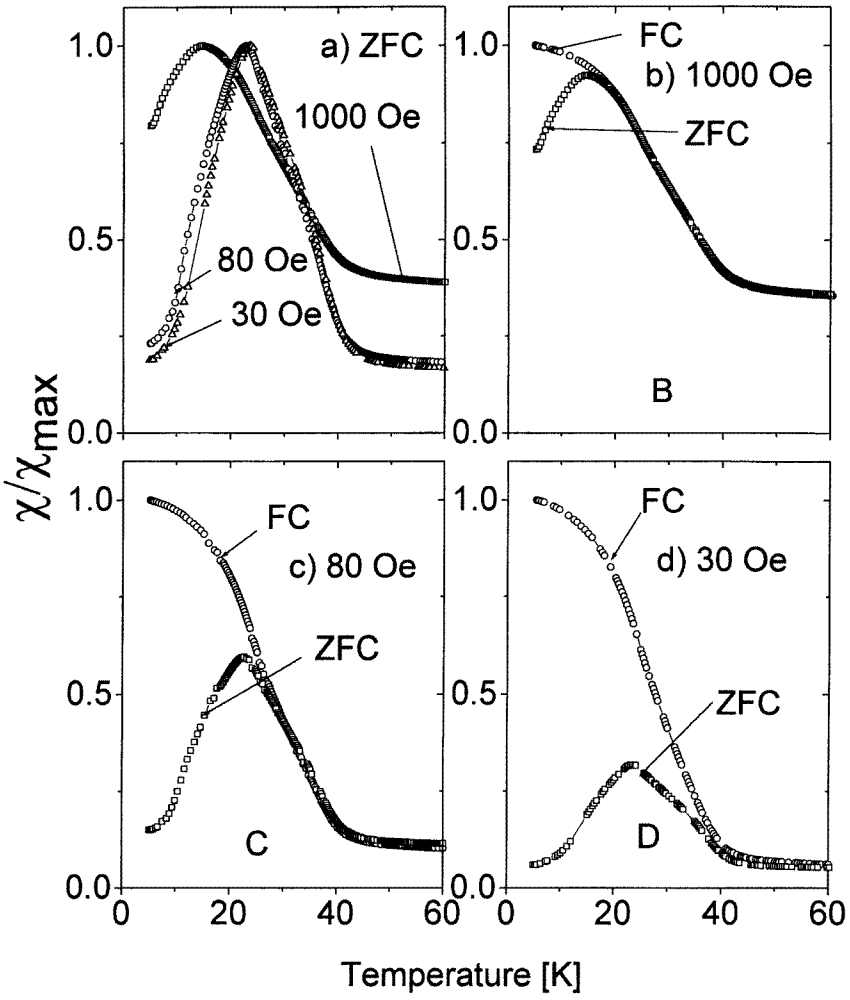

Figure 5. The temperature dependence of the magnetic susceptibility $\chi(T)$ relative to its maximum value χ_{max} in measuring fields $H = 30$, 80 and 1000 Oe, for the sample Cr+3.1% Mn in the ZFC and FC states: (a) in the ZFC state for three different fields; (b), (c) and (d) in both the ZFC and FC states for 1000, 80 and 30 Oe, respectively.

example, is proportional to the Mn concentration for $x \leqslant 0.5\%$ Mn and then varies roughly as $x^{2/3}$ until clusters of Mn atoms dominate the behaviour for $x > 10\%$. Furthermore, the decrease in $\chi(T)$ above T_f approaches a CW law (beyond about $5T_f$ in CuMn: see figure 3.1 in [4]) that corresponds to the thermal fluctuations of the moments on the impurity atoms.

The behaviour in the $Cr_{1-x}Mn_x$ system is strikingly different. The pinning temperature T_p, whose definition is illustrated in figure 4(d), is essentially independent of x. On the other hand, the peak temperature shows no systematic variation with x, and is believed to have no particular significance. Furthermore, above T_p the susceptibility $\chi(T)$ for samples containing $x \leqslant 6.2\%$ Mn soon becomes essentially independent of temperature

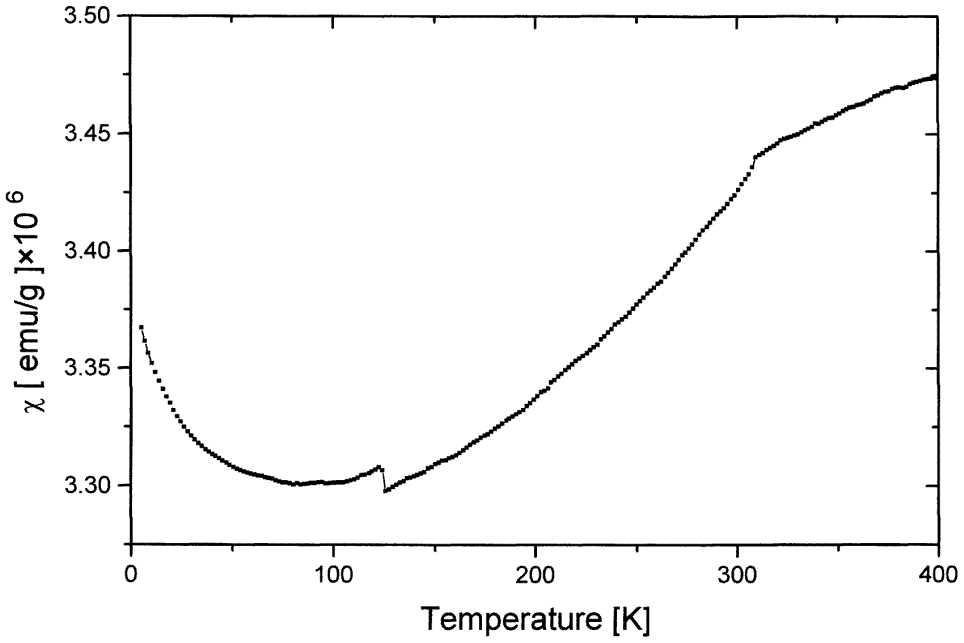

Figure 6. The temperature dependence of the magnetic susceptibility $\chi(T)$ of pure Cr with measuring field $H = 1000$ Oe.

up to considerably higher temperatures, while the appearance of CW paramagnetism at higher concentrations of Mn is accompanied by a *decrease* of the spin-glass component (see figure 3).

The relaxation of the magnetization at low temperature for two samples is shown in figure 9. It is characteristic of a spin glass that the relaxation from the FC state, as in figure 9(a), is considerably slower than that from the ZFC state, as in figure 9(b) [4]. These are preliminary measurements, and we plan to study relaxation effects systematically in our $Cr_{1-x}Mn_x$ samples.

The hysteresis on temperature cycling between the ZFC and FC states becomes more pronounced as the measuring field H decreases, as seen in figure 5. For $H = 30$ Oe, the irreversibility limit, where the ZFC and FC curves separate, is essentially at the pinning temperature. The progressive decrease of the irreversibility limit as the field increases from 30 to 80 Oe and then to 1000 Oe, seen in figure 5, suggests that the failure to observe hysteresis in previous studies [1] was due to the use of too large a measuring field, $H = 2.4$ kOe. We note also in figure 5(a) that the peak in $\chi(T)$ for the ZFC state becomes more rounded at higher fields, while the peak temperature decreases.

The field dependence of the magnetization $M(H)$ measured at 5 K is nonlinear and exhibits hysteresis for all concentrations of Mn at fields less than about 3 kOe, as illustrated in figure 10. The parameters of the magnetic hysteresis are given in table 2. The coercive field H_c in our CrMn samples peaks at $x = 1.5\%$ Mn, while both the remanent magnetization M_r in zero field and the value M_{ex} obtained by extrapolation from high fields are a maximum for $x = 3.1\%$ Mn. For concentrations $x \leqslant 11.2\%$ Mn, the field dependence of $M(H)$ is linear beyond about $H \simeq 3$ kOe. The high-field differential susceptibility $\mathrm{d}M/\mathrm{d}H$ is

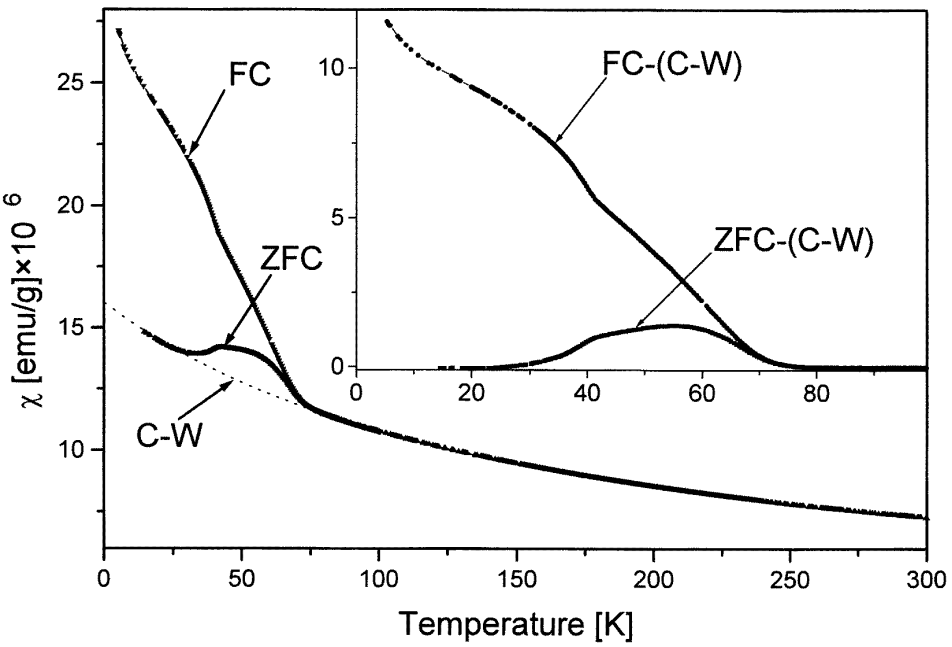

Figure 7. The temperature dependence of the magnetic susceptibility $\chi(T)$ of the alloy Cr+13.5% Mn, measured in the ZFC and FC states, with measuring field $H = 30$ Oe. The curve CW shows the fit of $\chi(T)$ to a CW law for temperature $T > 75$ K, extrapolated by the dashed line to lower temperatures. The inset shows the resultant spin-glass contribution to $\chi(T)$ obtained by subtracting the CW component.

Table 2. Parameters characterizing the field dependence of the magnetization $M(H)$ of alloys $Cr_{1-x}Mn_x$ at temperature 5 K in the range $-55 \leqslant H \leqslant 55$ kOe.

x % Mn	H_c (Oe)	M_r (10^{-4} emu g^{-1})	M_{ex} (10^{-4} emu g^{-1})	dM/dH (10^{-6} emu g^{-1})
$\ll 0.1$	55	1.4	5	2.96
0.6	280	10	18	2.94
1.5	520	42	78	2.80
3.1	220	72	197	2.97
4.6	130	47	169	2.98
6.2	100	30	157	3.11
7.7	100	40	190	4.47
10.1	90	16	130	5.7
11.2	90	23	70	5.8
13.5	12	1	—	21.3
14.7	—	—	—	20.0
19.4	—	—	—	18.8

essentially the same as the value for pure Cr at low temperatures, but for $7.7 \leqslant x \leqslant 11.2\%$ Mn it is up to a factor of two larger (see table 2).

The nature of the field dependence of $M(H)$ changes drastically between the compositions $x = 11.2$ and 13.5% Mn, as illustrated in figure 10(b) (see also figure 5 in [1]). The hysteresis disappears almost completely for $x \geqslant 11\%$ Mn, and the differential

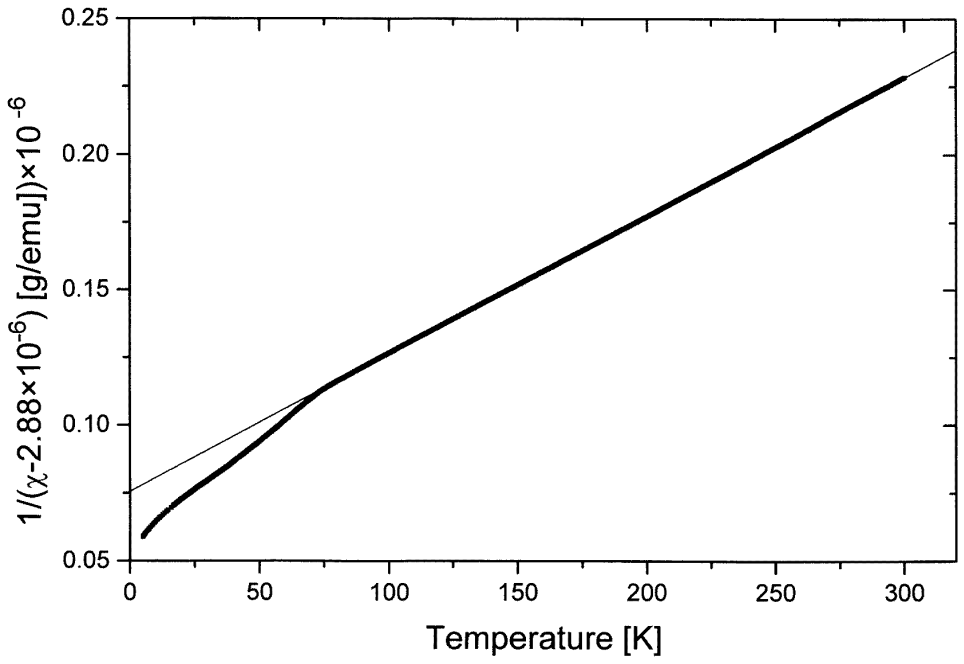

Figure 8. The fit of the temperature dependence of the magnetic susceptibility $\chi(T)$ of the Cr+13.5% Mn sample shown in figure 7 to a CW law, over the temperature interval $75 \leqslant T \leqslant 300$ K. The CW parameters are given in table 1.

susceptibility $\mathrm{d}M/\mathrm{d}H$ increases by almost a factor of four. We note that in fact the magnetization is nonlinear at high fields in these samples, and in table 2 only the lower-field values are given, the higher-field values being about 10% smaller.

4. Discussion

We have seen that CrMn alloys exhibit behaviour characteristic of a spin glass, but with important differences. Thus a peak in the temperature dependence of the magnetic susceptibility, with irreversibility with respect to zero-field cooling and field cooling, the irreversibility limit moving to higher temperatures as the measuring field increases, are strong indicators of a spin glass. The relaxation as a logarithm of time, slower from the field-cooled than from the zero-field-cooled state, is another characteristic feature of a spin glass. There is also hysteresis with respect to field cycling.

On the other hand, the lack of dependence of the characteristic temperature of the peak on the Mn content of the alloy is completely different from the behaviour of a typical metallic spin glass, in which the magnetic atoms couple by the RKKY interaction. Furthermore, the susceptibility is independent of temperature above the pinning temperature, which is why we choose to describe this, rather than the peak, as the characteristic temperature. In a typical metallic spin glass, the peak defines the freezing temperature, where thermal fluctuations of spins abruptly cease and the system enters a state of frustration, so that the CW paramagnetism gives way to a susceptibility that decreases as the temperature decreases. In CrMn, which exhibits Pauli paramagnetism at higher temperatures, some process as yet

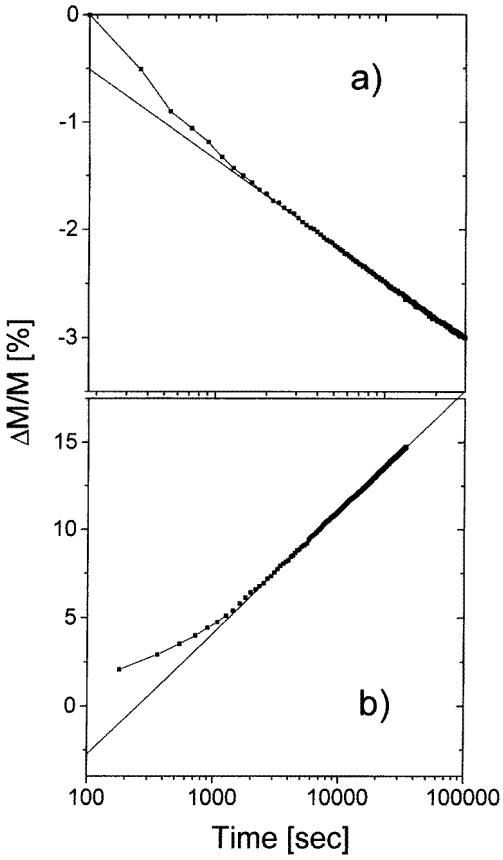

Figure 9. Relaxation of the magnetization $M(t)$ with time t at temperature 5 K: (a) Cr+1.5% Mn field cooled in a magnetic field $H = 10$ kOe, with measuring field $H = 80$ Oe, the fit to the data beyond about $t = 5000$ s being $\Delta M/M\% = 2.20 - 1.13\log(t)$; and (b) Cr+4.6% Mn cooled in zero magnetic field, with measuring field $H = 80$ Oe, the fit to the data beyond about $t = 5000$ s being $\Delta M/M = -17 + 69\log(t)$.

not understand begins at the pinning temperature.

We are led to propose that we have here a new type of spin glass in which the presence of Mn is necessary, but the interaction between the Mn moments is not responsible for the frustration. In [3] we proposed a model that assumes the existence of a frozen moment M on a single Mn impurity atom in the Cr host. The moment of about 4 μ_B on the Mn atom responsible for the CW temperature dependence of $\chi(T)$ in the paramagnetic phase evidently freezes at the Néel transition, since in alloys containing up to about 4% Mn the susceptibility in the SDW phase is only weakly dependent on temperature, just as in pure Cr [1, 2]. We postulate that M is oriented along the same cube axis as the moment m of the Cr atom for which the Mn atom substitutes, or along the polariztion direction of the SDW in the incommensurate SDW phase. The direction of M at higher temperatures may however be either parallel or antiparallel to m, the latter corresponding to a metastable configuration. The magnetic anisotropy will increase in magnitude as temperature decreases, and we suppose further that the energy of the antiparallel configuration increases faster than that of neighbouring orientations, so that at some temperature T_p this configuration becomes

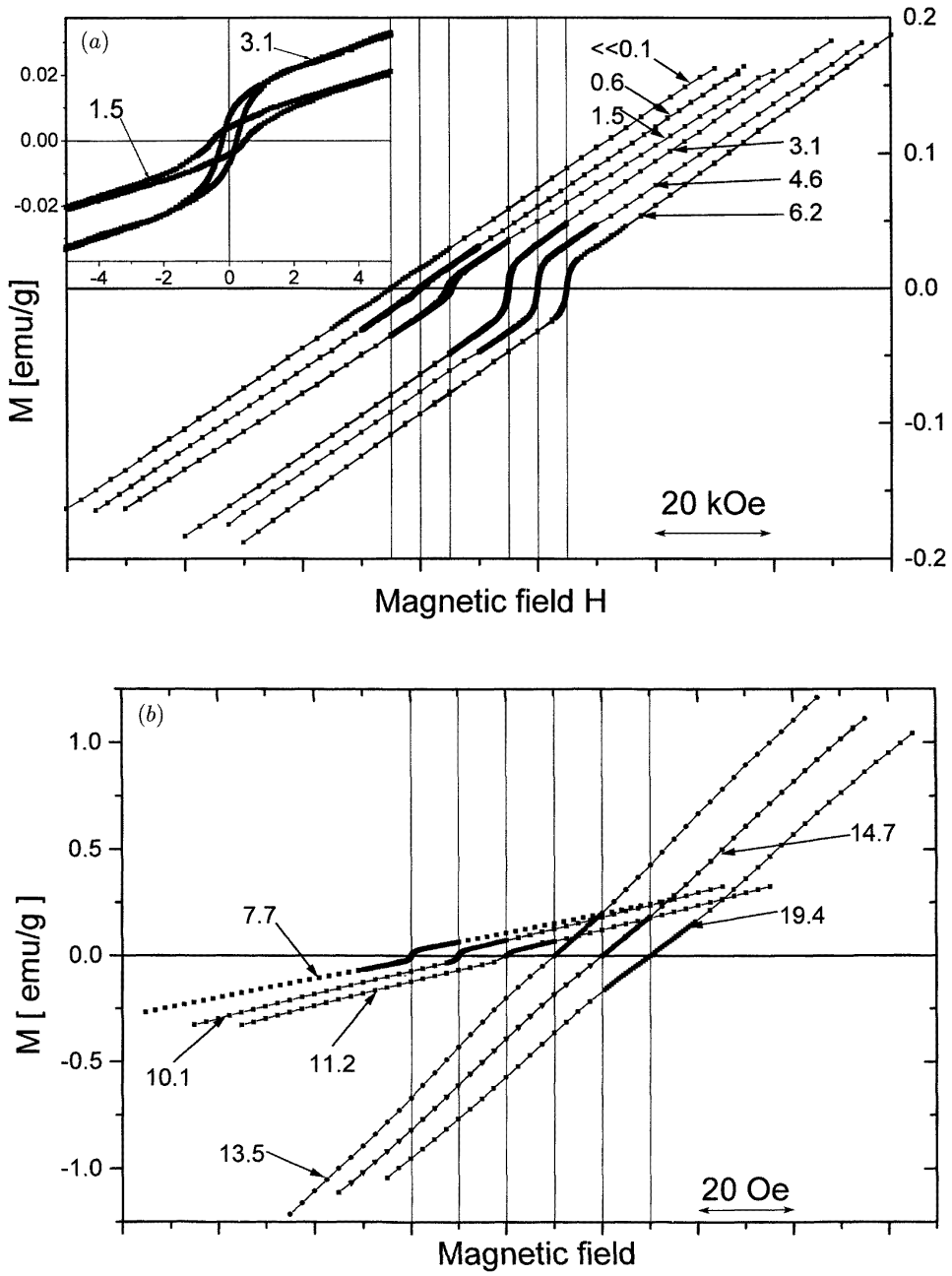

Figure 10. The magnetic field dependence of the magnetization $M(H)$ of $Cr_{1-x}Mn_x$ alloys at temperature $T = 5$ K: (a) lower-concentration alloys, $x \leqslant 6.2\%$ Mn, with the inset showing hysteresis for two of the samples with expanded scales; and (b) higher-concentration alloys, $7.7 \leqslant x \leqslant 19.4\%$ Mn. The curves are labelled with the concentration of Mn, x%.

unstable. At this pinning temperature the directions of the Mn moments remain unchanged, but this phase of the SDW changes by π so as to make $m \parallel M$, i.e., to make M antiparallel to the moments of its Cr neighbours.

Considering now the relative directions of M on two neighbouring Mn atoms, in some cases there will be frustration of Cr atoms on a surface between them, resulting from the competition between the two polarization directions of the SDW required for the moment of the Cr atom to be in phase with one or the other. When all the Mn atoms are thus considered, they will be seen to partition the SDW into phase domains that surround each Mn atom (or pair of atoms or more whose moments are in phase with each other), the different domains being separated by surfaces of frustration of the moments of the Cr atoms.

These frustrated moments on the Cr atoms are responsible for the increase in $\chi(T)$ below the pinning temperature, $T_p \simeq 40$ K, in dilute $Cr_{1-x}Mn_x$ alloys. As x increases, however, the number of pairs, triplets, and higher-order clusters will grow at the expense of the single Mn atoms, and the frustration surfaces will eventually disappear. This model might be appropriate at low concentrations of Mn in $Cr_{1-x}Mn_x$, say $x = 0.6\%$ Mn, where the average spacing between the Mn atoms in a bcc lattice is ten lattice constants. It is difficult, however, to envisage its application to the higher-concentration alloys, say $x = 8\%$ Mn, where on average each Mn atom has one Mn neighbour.

It we consider alloys in which the Mn concentration is greater than about 2%, so that at low temperature the SDW is commensurate with the lattice [4], we might speculate that polarization domains exist, in which the Cr moments are directed along one of the three crystal axes, as the polarization of the incommensurate SDW does in pure Cr [7]. The enhanced susceptibility at low temperatures might then be a manifestation of the frustration of the Cr moments at the boundaries between the polarization domains, which in some way is mediated by the Mn moments. It is difficult to see, however, why the frustration should start abruptly at a pinning temperature that is independent of Mn concentration. It should be noted also that the magnitude of the peak in the susceptibility is about two orders of magnitude smaller than what would be expected for the frustration of a single Cr atom for every Mn atom.

The fact that the pinning temperature of the sample containing only a trace of Mn is roughly the same as in those containing much higher concentrations of Mn (see figure 4, which indicates a value, $T_p \simeq 60$ K, for this sample, and table 1) is in strong contrast with the behaviour of a typical spin-glass system. We estimate from the fact that the Néel temperature T_N for this sample is the same as that for pure Cr to a precision of about 1 K, and from the temperature dependence of T_N upon x in dilute $Cr_{1-x}Mn_x$ alloys, $dT_N/dx = 50$ K/% Mn [10], that $x < 0.02\%$ Mn. It is noteworthy that in the prototypical $Cu_{1-x}Mn_x$ system the freezing temperature of the spin glass is only about 0.1 K for this concentration of Mn (see figure 4.2 in [4]).

We note also that nominally pure Cr shows no sign of spin-glass behaviour like that seen in CrMn alloys. Thus four Cr samples of different provenance showed no difference in behaviour after field cooling in the measuring field, $H = 30$ Oe. All showed, however, a low-temperature anomaly, as seen in figure 6 for one of the samples. The susceptibility increases by a small amount but ever more rapidly as temperature decreases below about 80 K. Other workers have reported, without comment, similar behaviour [2, 11–14].

Another strong contrast between the behaviour of CrMn and typical spin-glass alloys is the relatively small deviation in the former of the magnetization $M(H)$ from linearity in the field H, as seen in figure 10. These magnetization curves should be compared with those for CuMn alloys, which show very strong nonlinearity at high fields (see figure 3.29 in [4]).

The onset of CW paramagnetism in $Cr_{1-x}Mn_x$ alloys above the pinning temperature as x increases beyond about 7% Mn, with Pauli paramagnetism for lower concentrations, may perhaps be related to atomic short-range order (ASRO) of the Mn atoms. Thus in $Ag_{1-x}Mn_x$ alloys the second-nearest neighbours are ferromagnetically correlated, whereas nearest-neighbour Mn atoms are antiferromagnetically correlated, and the CW temperature accordingly changes from positive to negative values with increasing x between about $x = 21$ and 28% Mn [15]. The relatively large number of second-nearest neighbours for two samples containing $x = 13$ and 21% Mn due to ASRO, as determined from x-ray intensity measurements, thus gives rise to the large ferromagnetic CW temperatures for these concentrations of Mn in $Ag_{1-x}Mn_x$ alloys.

The fact that the amplitude of the spin-glass peak in $Cr_{1-x}Mn_x$ increases initially with increasing x at low concentrations of Mn, reaches a maximum value at about $x = 5\%$ Mn, and thereafter decreases, as seen in figure 3(a), suggests that it is associated with single Mn atoms with all eight neighbours being Cr. When CW paramagnetism appears above the pinning temperature for $x \geqslant 7.7\%$ Mn, the CW temperature T_0, given in table 1, is large and negative, which indicates antiferromagnetic coupling of the Mn moment with the local magnetization.

The magnetization $M(H)$ becomes nonlinear at high fields for $x \geqslant 11.2\%$ Mn, as may just be seen in figure 10(b), though a plot of $\mathrm{d}M/\mathrm{d}H$ versus H makes this effect clearer. This indicates that clusters of Mn atoms appear, between which there is ferromagnetic coupling [16]. Nevertheless, the CW temperature remains large and negative (table 1), which indicates that antiferromagnetic coupling is dominant. We note further that in an alloy of 13.5% Mn in Ag, where the coupling is ferromagnetic, the susceptibility at temperature 40 K is about fifty times larger than in Cr+13.5% Mn [15].

In a typical metallic spin-glass such as CuMn, $M(H)$ is nonlinear at high fields even in dilute alloys (see figure 3.29 of [4]). This is because the field has to overcome an array of randomly oriented anisotropy axes before the various clusters of spins can align along the field direction giving saturation at very high fields. These clusters exist even at low concentrations of Mn due to the long range of the RKKY interaction. In CrMn alloys, on the other hand, one might expect the crystal anisotropy to be the same as that in pure Cr, i.e., the easy axis along one of the cubic axes.

The abrupt increase in the Curie constant in $Cr_{1-x}Mn_x$ alloys between $x = 11.3$ and 13.5% Mn (see table 1) is no doubt associated with ASRO, with the formation of large moments associated with ferromagnetically coupled clusters of Mn atoms. This interesting behaviour encourages studies of x-ray intensity and diffuse-neutron scattering in $Cr_{1-x}Mn_x$ alloys.

Finally, we note the small anomaly in the temperature dependence of the susceptibility at a temperature of about 20 K in the field-cooled state of samples of $Cr_{1-x}Mn_x$ in the range $4.6 \leqslant x \leqslant 11.2\%$ Mn (see figures 1(a) and 4). The same anomaly was observed by Maki and Adachi (see figure 6 of [1]) in the range $2.2 \leqslant x \leqslant 14.7\%$ Mn. They suggested that the anomaly is due to some kind of spin reorientation in the spin-density wave. This explanation seems unlikely, but we have no alternative to offer.

Acknowledgments

This work was performed with partial support by Conselho Nacional de Desenvolvimento Cientifico e Tecnologgico—CNPq (VYuG and PCdeC), and the Natural Sciences Engineering Research Council of Canada (EF).

References

[1] Maki S and Adachi K 1979 *J. Phys. Soc. Japan* **46** 1131
[2] Aidun R, Arajs S and Moyer C A 1985 *Phys. Status Solidi* b **128** 133
[3] Galkin V Yu, de Camargo P C, Ali N, Schaf J and Fawcett E 1995 *J. Phys.: Condens. Matter* **7** L649
[4] Mydosh J A 1933 *Spin Glasses: An Experimental Introduction* (London: Taylor and Francis)
[5] Sternlieb B J, Lorenzo E, Shirane G, Werner S A and Fawcett E 1994 *Phys. Rev.* B **50** 16 438
[6] de Oliviera A J A, de Lima O F, Ortiz W A and de Camargo P C 1995 *Solid State Commun.* **96** 383; 1995 private communication
[7] Fawcett E 1988 *Rev. Mod. Phys.* **60** 209
[8] Greerken B M, Griessen R, Benediktsson G, Astrom H U and van Dijk C 1982 *J. Phys. F: Met. Phys.* **12** 1603
[9] Kondorskii E I, Kostina T I and Galkin V Yu 1978 *The Physics of Transition Metals (Inst. Phys. Conf. Ser. 39)* ed M J G Lee *et al* (Bristol: The Institute of Physics) p 611
[10] Fawcett E, Alberts H L, Galkin V Yu, Noakes D R and Yakhmi J V 1994 *Rev. Mod. Phys.* **66** 25
[11] Ishikawa Y, Tournier R and Filippi J 1965 *J. Phys. Chem. Solids* **26** 1727
[12] Chiu C H, Jericho M H and March R H 1971 *Can. J. Phys.* **49** 3010
[13] Bender D and Müller J 1970 *Kondens. Mater.* **10** 342
[14] Koebler U and Dubiel S M 1987 *Z. Phys.* B **61** 247
[15] Koga Kenji, Ohshima Ken-ichi and Niimura Nobuo 1993 *Phys. Rev.* B **47** 5783
[16] Rizzuto C 1974 *Rep. Prog. Phys.* **37** 147